J Appl Electrochem (2012) 42:435–442
DOI 10.1007/s10800-012-0417-1

ORIGINAL PAPER

Application of in situ electrochemically generated ozone for degradation of anthraquninone dye Reactive Blue 19

J. Basiri Parsa · M. Abbasi

Received: 5 February 2012 / Accepted: 12 April 2012 / Published online: 25 April 2012

Abstract Degradation of anthraquninone dye C.I. Reactive Blue 19 (RB19) via generated ozone by electrochemical oxidation process was investigated in this research. Ti/Sn–Sb–Ni electrode was used as an anode for ozone generation. The anode electrode was characterized electrochemically by cyclic voltammetry and characterized morphologically by scanning electron microscopy and X-ray diffraction. The amount of ozone concentration and RB19 degradation increased with increasing of applied voltage, electrolysis time, and in 1 M $HClO_4$ at room temperature. The results of UV/Vis spectroscopy showed that the anthraquinone structure was degraded by dissolved generated ozone and also intermediate compounds were detected by integrated gas chromatography–mass spectrometry (GC/MS). Removal of color and COD were 100 % after 3 min and 48.2 % after 15 min reaction time, respectively.

Keywords Electrochemical oxidation · Generated ozone · Degradation · Reactive Blue 19

1 Introduction

The strategies for environmental protection in industry generally include processes for waste water treatment as well as development of new processes or products which have little or no harmful effects on the environment [1]. Large amounts of chemically different dyes are produced annually around the world. They are used extensively in the dye and printing industries, and 5–10 % of the dyestuffs are lost in the industrial effluents [2, 3]. In the past, colorant wastewaters were treated by conventional methods, such as biological oxidation [4] and adsorption [5, 6]. Recently, chemical oxidation (use of chlorine, ozone, hydrogen peroxide, and wet air oxidation), electrochemical technology [7, 8], sonolysis [9, 10], and advanced oxidation processes (AOP) (Fenton's reaction, ozone + UV radiation, and photochemistry) are currently used to treat industrial effluents [11, 12].

AOP are the most powerful methods for degradation of textile wastewater [13, 14]. It is well known that ozone is a strong oxidant which can form a more powerful oxidizing agent. Owing to this high oxidation potential, ozone can effectively break down the conjugated double bonds of dye chromophores and other functional groups, such as the complex aromatic rings of dyes. Subsequent formation of smaller nonchromophoric molecules decreases the color of the effluents [15–17].

The extending of application is attributed to oxidizing properties of O_3. Ozone provides green oxidation when decomposition of ozone leads to environmentally friendly products (O_2) [16]. Electrochemical oxidation is more advantageous than the classic corona method for ozone production because of, for example, high concentrations in the gas and liquid phases, simple system design, and low voltage operation**.** In the electrochemical process, ozone is generated at the anode surface. However, ozone generation severely competes with O_2 evolution which is thermodynamically favorable. (see Eqs. 1–3) [18].

$$O_3 + 6H^+ + 6e^- \rightleftarrows 3H_2O \quad E^\circ = \quad 1.51 \text{ V vs. RHE} \quad (1)$$

$$O_3 + 2H^+ + 2e^- \rightleftarrows H_2O + O_2 \quad E^\circ = 2.07 \text{ V vs. RHE} \quad (2)$$

J. B. Parsa (✉) · M. Abbasi (✉)
Faculty of Chemistry, Bu-Ali Sina University,
65178 Hamedan, Iran
e-mail: parssa@basu.ac.ir

M. Abbasi
e-mail: mahabbasi79@yahoo.com

$$O_2 + 4H^+ + 4e^- \rightleftarrows 2H_2O \quad E^\circ = 1.23 \quad V \text{ vs. RHE} \qquad (3)$$

The inhibition of O_2 evolution is a first requirement for an efficient generation of O_3 at a reasonable current [19]. Thus, materials for electrochemical generation of ozone must have a high overpotential of oxygen evolution and they should also be stable to strong anodic polarization in the electrolyte [20, 21].

Application of ozone (O_3) as an oxidant for degradation of dyestuff pollutants has been used by several researchers [22–26]. It is evident that ozonation can achieve high color removal, reduce organic compounds, improve biodegradability, and ensure effective disinfection without byproduct residuals. Ozonation for decolorizing dyestuff wastewater has the following advantages: (1) It does not increase the volume of wastewater and sludge; (2) It removes color and reduces the organic matter in one step; (3) It needs little space, and it is easily installed on a site; (4) It is less harmful than other oxidative processes because it has no stock hydrogen peroxide or other chemicals that are required on a site; (5) Residual ozone can be easily decomposed to oxygen [27, 28].

Reactive Blue 19 (RB19) is a model anthraquinone reactive dye. A few past researches concerned with ozonation of RB19 solution were focused on degradation efficiency and color removal [29]. Fanchiang and Tseng [27] have reported the transformation of RB19 under different ozonation conditions in 10 min of reaction time and found that partial oxidation was obtained as well as Ozone gas was generated from pure oxygen by the ozone generator with classic corona method for degradation of RB19.

The aim of the present study is to investigate the degradation of the RB19 by in situ electrochemical-generated ozone in acidic media at room temperature. Effects of coating times, electrolyte type, electrolyte concentration, applied voltage, and initial dye concentration have been optimized.

2 Experimental

2.1 Electrode preparation

A titanium mesh (25 × 25 mm^2) was degreased with acetone, rinsed in Millipore water, contacted with boiling oxalic acid for 1 h, and cleaned in an ultrasonic bath in Millipore water for 1 h. Metal salts, $SnCl_4 \cdot 5H_2O$ (98 %, Sigma Aldrich), $SbCl_3$ (99.5 %, Sigma Aldrich), and $NiCl_2 \cdot 6H_2O$ (98 %, Merck), were dissolved in absolute ethanol, after which concentrated HCl was added dropwise until the solution was clear. The titanium mesh was coated by dipping process, followed by drying at 105 °C for 15 min, and then annealing at 520 °C for 25 min. This was repeated several times, in the last of which the annealing lasted for 1 h. The molar ratio of Sn–Sb–Ni was controlled to be 500/8/1 in the coating solution [18, 30].

2.2 Electrochemical ozone production

A commercial Ag/AgCl electrode was used as a reference electrode and platinized titanium (electrodeposition of H_2PtCl_6 on the Ti mesh (2.5 × 2.5 cm^2)) as counter electrode. All the experiments were performed in an undivided cell with volume 200 ml and in constant potential coulometer (CPC) (coulometer 2050, Behpajooh Company, Iran).The concentration of dissolved ozone and change of dye concentration were controlled using a UV/Vis spectrophotometer (Jusco, Japan). The UV spectrum was calibrated by the standard indigo method. For the spectrophotometer used, 1 mg L^{-1} dissolved ozone gave an absorbance of 0.098 at the wavelength of 258 nm [18, 30].

2.3 Materials and apparatus

The commercial anthraquinone reactive dye RB19 was purchased from Alvan Sabet Co., Iran and used without any purification. Before the ozonation experiments, a RB19 dye stock solution (200 mg L^{-1}) was prepared and then diluted with deionized water. Chemical oxygen demand (COD) was measured to investigate the mineralization of the substrate, using a closed reflux digester reactor (HACH, DRB 200) and the corresponding spectrophotometer (HACH, DR 2800). SEM observation was performed on LEO 1455 VP (LEO Electron Microscopy) Ltd scanning microscope). The cyclic voltammetry experiments were conducted using a three-electrode cell, with Platinum wire as the counter electrode, and Ag/AgCl as the reference electrode, and Ni–Sb–SnO_2/Ti electrode (1 cm × 1 cm) as the working electrode. CV curves of the testing anodes were produced by potentiostat/galvanostat ATOLABS (The Netherlands). X-ray diffraction (XRD) patterns of the coating films were recorded on a XRD instrument (Siemens D5000, XRD), with an operating voltage of 40 kV, current of 30 mA, and 2θ = 10–85°.

2.4 GC/MS analysis

Intermediate compounds were detected by gas chromatography coupled with mass spectrometry (GC 2010/MS, Shimadzu, Japan). The GC system was equipped with a capillary chromatographic column (30 m × 0.25 mm, 0.25 μm). The injection was conducted on a splitless mode, and injector temperature was 250 °C with helium serving as the carrier gas at the flow rate of 0.8 mL min^{-1}. The extracted temperature samples were chromatographed under the following gradient; initial column temperature was held constant at 40 °C for 10 min, increased at the rate of 12 °C

min^{-1} up to 100 °C, then ramped at 5 °C min^{-1} to 200 °C, further ramped at 20 °C min^{-1} to 270 °C and kept constant for 5 min, and then raised at the rate of 10 °C min^{-1} up to 300 °C, and finally maintained constant for 5 min [31].

3 Result and discussion

3.1 Electrochemical ozone production

The usage of Ti/Sn–Sb–Ni electrode as anode has a high overpotential for the oxygen evolution reaction when this electrode combined with a supporting electrolyte at room temperature can obtain high concentration of ozone by electrochemical oxidation process and also its application for degradation of RB 19 is reported in the article. The cyclic voltammograms (CVs) of the anode are shown in Fig. 1. The CV was performed at 50 mV s^{-1} at different acid types at room temperature. The onset potential is close to 1.85 V versus Ag/AgCl, and it was much higher than the typical value expected for oxygen evolution which is 1.02 V versus Ag/AgCl in acid solution, indicating that oxygen evolution was kinetically suppressed.

Within the scanned voltage range, CVs of the electrodes did not have any peaks or shoulders, and further, there was no cathodic current on the reverse scan. Morphologically character was observed with a scanning electron microscopy (SEM) and XRD. The crystal size and the structure of the composite are important factors for the efficiency of the anode, especially when the crystal size is decreased to the nanoscale. In Fig. 2, XRD spectra show that the average particle size of composite, L, was under 10 nm, and it was confirmed in SEM images, see Fig. 3. The average grain sizes were calculated by Scherrer equation:

$$L = \frac{k \cdot \lambda}{\mathrm{FWHM} \cdot \cos\theta} \quad (4)$$

In Eq. (4), L is average grain size (nm), k is Scherrer constant, λ is the wavelength of X-ray, FWHM is obtained from the diffraction peak width at half maximum, and θ is the diffraction angle (rad).

Figure 3 clearly shows the difference of electrodes surface, with and without coating. Also, images are shown with coated electrode that has more active surface than the neat one.

The effect of applied voltage on the ozone generation was showed in Fig. 4a, The results show an optimal potential of 2.4 V versus Ag/AgCl with the highest concentration of ozone 24.4 mg L^{-1} after 10 min (600 s) electrolysis time. The results show that ozone concentration decreased when we increased the applied voltage after 2.4 V versus Ag/AgCl. This decline may be increase the competing side reaction of oxygen evolution or increase the ohmic losses due to lower conductivity in the solution when the gas bubbles were generated.

Ozone concentration was found to differ in different acidic media. The type of acid as an electrolyte would directly affect proton concentration. The effect of the acid type on ozone production was investigated. Three acids: perchloric acid, sulfuric acid, and phosphoric acid were used, representing anions of different valence charges. Figure 4b shows that the effect of acid concentration was similar for the three acids. The highest ozone concentration was achieved in $HClO_4$, and the lowest was found in H_3PO_4. The original reaction of H_2SO_4 is a formation of peroxodisulfuric acid due to the oxidation of the sulfuric acid. In contrast, the main reaction of $HClO_4$ is oxygen evolution due to water oxidation. As shown in Fig. 4c, ozone concentration has increased to 27 mg L^{-1} after 20 min (1,200 s) of electrochemical oxidation process time. The dissolved ozone concentration depended on the applied voltage, concentration, and type of electrolyte.

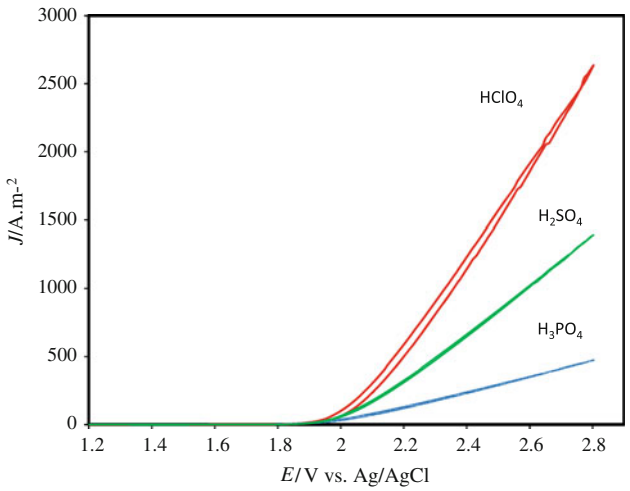

Fig. 1 Cyclic voltammetry curves obtained at different acid types in 1 M concentration. Potential scan rate, 50 mV s^{-1}, platinum wire as the counter electrode, and Ag/AgCl as the reference electrode, and Ni–Sb–SnO_2/Ti electrode as the working electrode

3.2 Degradation and decolorization of RB19

Figure 5 shows the absorbance reduction of RB19 solution in the UV/VIS spectra at the generated ozone during the reaction time. In general, for UV/VIS light absorption, RB19 dye has two major absorption bands: one is in the UV region of 258 nm which characterizes the anthraquinone structures (the chromophore components of the dye molecules), and the other is in visible region of 592 nm, which corresponds to the blue color. Figure 5 shows that the absorbance reduction at these two characteristic wavelengths gradually

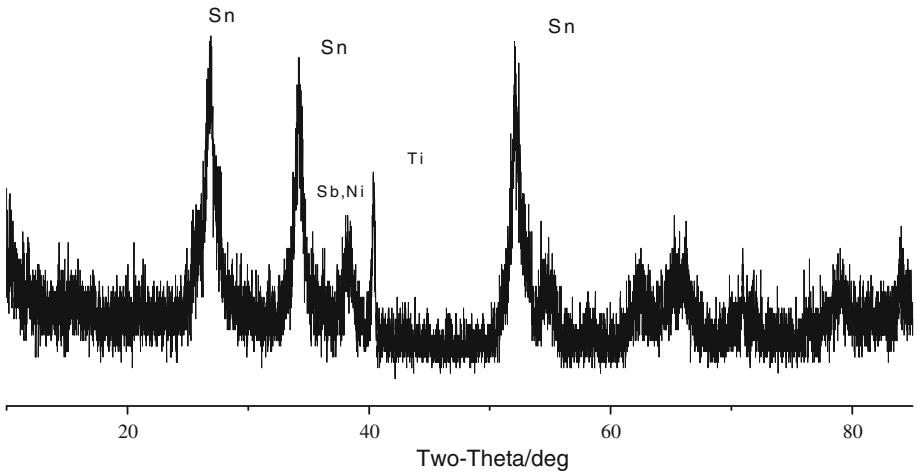

Fig. 2 XRD spectra of the Ti/Sn–Sb–Ni

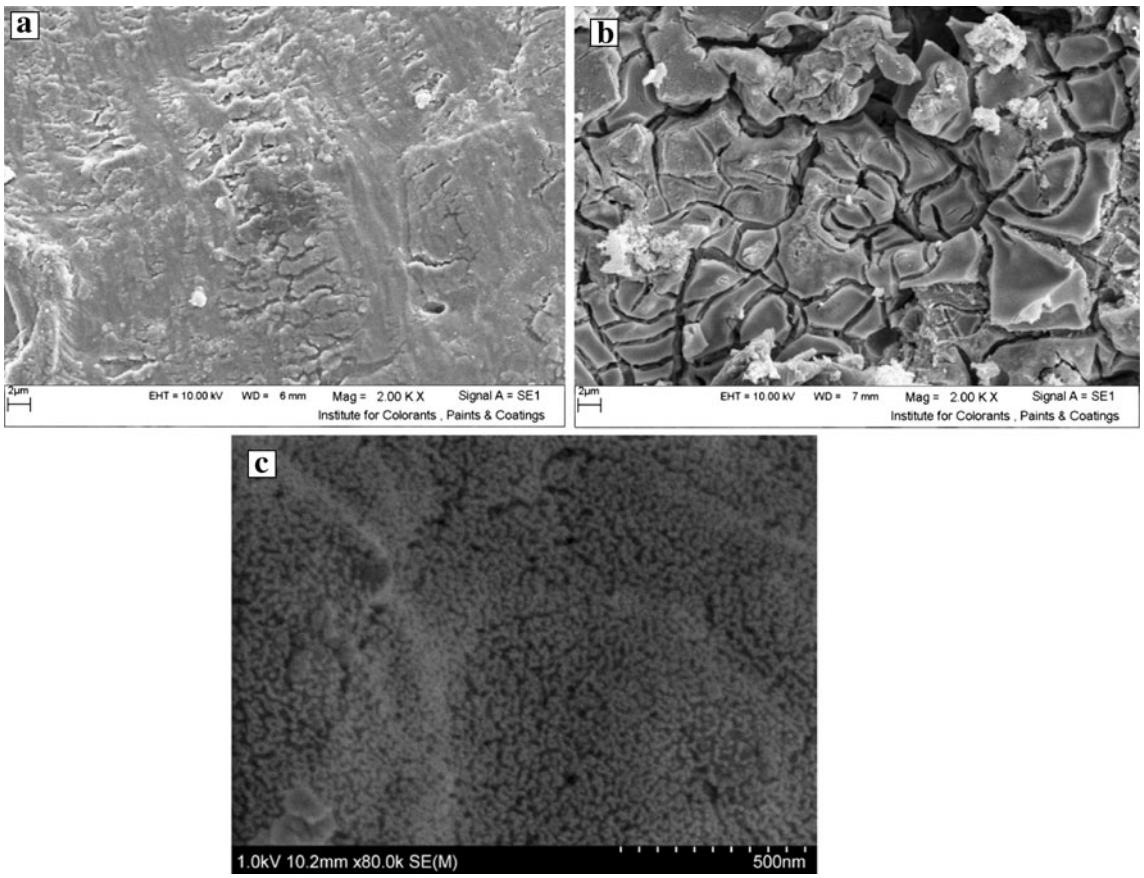

Fig. 3 SEM images Ti/Sn–Sb–Ni (**a**) surface of net titanium without coating (**b**, **c**) with coating

decreased with the increase of reaction time and reached almost 100 % at 3 min of ozonation process. Decline of absorption of RB19 at UV/Vis spectra in tow λ_{max} (258 nm and 592 nm) as shown in Fig. 5, caused to cleavage of chromophore and degradation of RB19 structure by ozone. The degradation of RB19 mainly related to the destruction of chromophore structures, and the rate was slower than decolorization that is involved only in the visible region.

The results of the GC/MS analysis in Fig. 6 and Table 1 also show that some intermediate products of RB19 solution were identified after 20 min of ozonolysis with electrochemically generated ozone. The matching degrees of

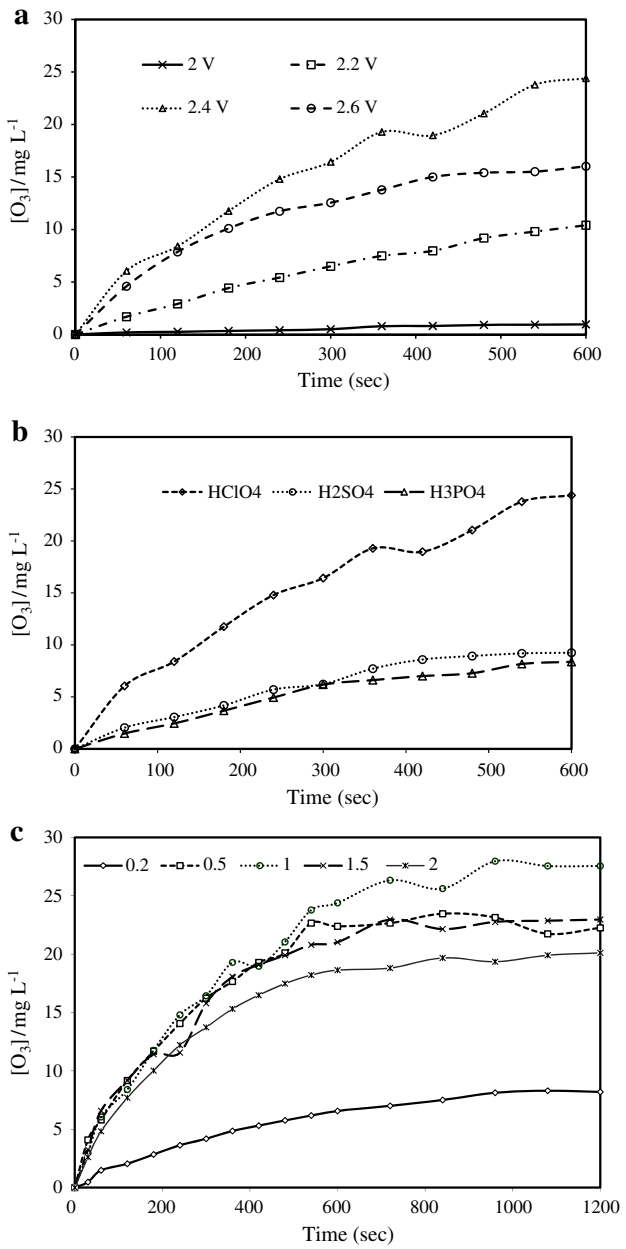

Fig. 4 Influence of important factors on the ozone generation: **a** effect of applied voltage, **b** effect of acid type and concentration, **c** concentrations of generated ozone in water versus the electrolysis time at different concentration of $HClO_4$

these products are comparable with NIST (127, 147), and the Wiley library ranged from 60 to 94 %.

The intermediate species acetic anhydride, propionic acid, 2, 4, 4-trimethyl-1 pentanol, hydroperoxide, 1-penten-3-one, dodcane, hexadecane, oxalic acid, and 1, 2-propadiene were detected. Results showed that most intermediate products are aliphatic compounds, although some of these compounds, such as 1-,2-,3-trimethyl benzene and 1,3 cyclohexandione were observed. Several intermediates are linear structures that have less harmful effects on the environment.

Table 1 Some intermediates identified after ozonolysis

Intermediates	Chemical formula	Molecular weight
Acetic anhydride (D1)	$C_4H_6O_3$	102
2,4-Di-tert-butylphenol	$C_{14}H_{22}O$	206
2-Propionic acid (D2)	$C_8H_{14}O_2$	142
1,2,3-Trimethyl benzene (D3)	C_9H_{12}	120
Dodecane (D4)	$C_{12}H_{26}$	170
Decane	$C_{10}H_{22}$	142
1,3-Cyclohexandione	$C_8H_{12}O_2$	140
2,4,4-Trimethyl-1-pentanol (D5)	$C_8H_{18}O$	130
Hydroproxide	$C_5H_{12}O_2$	104
1-Penten-3one	C_5H_8O	84
1,2-Propadiene (D6)	C_3H_4	40
Oxalic acid (D7)	$C_2H_2O_4$	90

3.3 Effect of initial dye concentration

The decolorization of RB19 solution was almost completed after 3 min ozonation time with inlet ozone concentrations of 27 mg L^{-1} at optimal condition. In order to study the feasibility of the generated ozone by electrochemical process for different concentrations of dye, experiments were carried out in acidic media by varying the initial concentration of dye from 25 to 100 mg L^{-1}. The effect of initial dye concentration on decolorization efficiency is shown in Fig. 7. As seen in this figure, by increasing the dye concentration, the decolorization rate is decreased. This could be because the ratio of generated ozone molecules to dye molecules in the solution decreases with the increase of the dye concentration. Increasing the initial dye concentration would result in more consumption of ozone. Also, in the oxidation process, with an increase in the dye concentration, various intermediates formed upon degradation of the dye may interfere with the oxidation [32]. Such repression would be clearer in the presence of an elevated level of degradation intermediates formed due to an increased dye concentration. Thus, the time for complete degradation and decolorization would be longer for higher initial dye concentrations. The percentage color removal of the parameters evaluated, decolorization and degradation, was determined using the following equation:

$$\text{Color removal}\,\% = \frac{(C_0 - C)}{C_0} \times 100 \qquad (5)$$

where C_0 and C are initial dye concentration and dye concentration at time t (min), respectively.

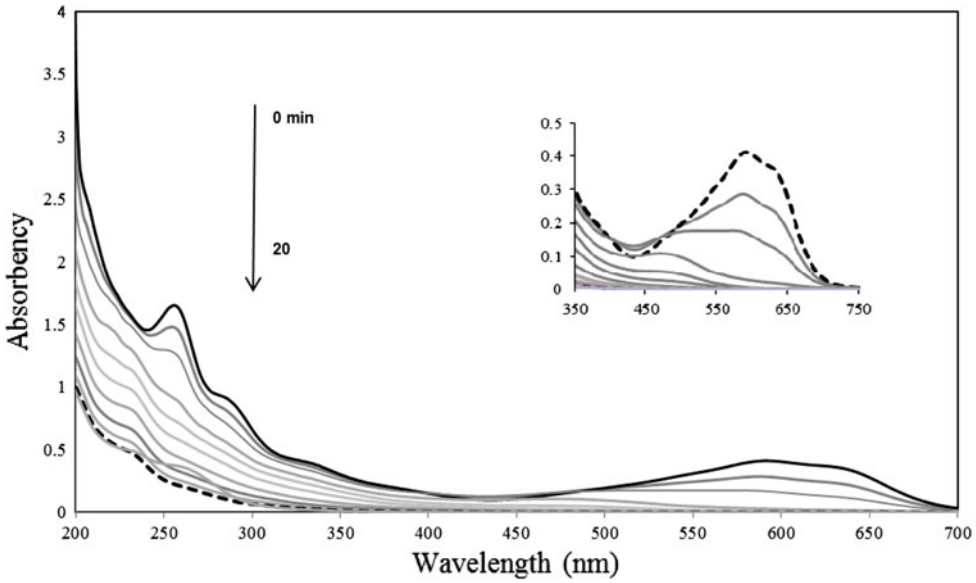

Fig. 5 Change in the absorption UV/Vis spectra of RB19 during of ozonolysis: initial dye concentration: 50 mg L^{-1}

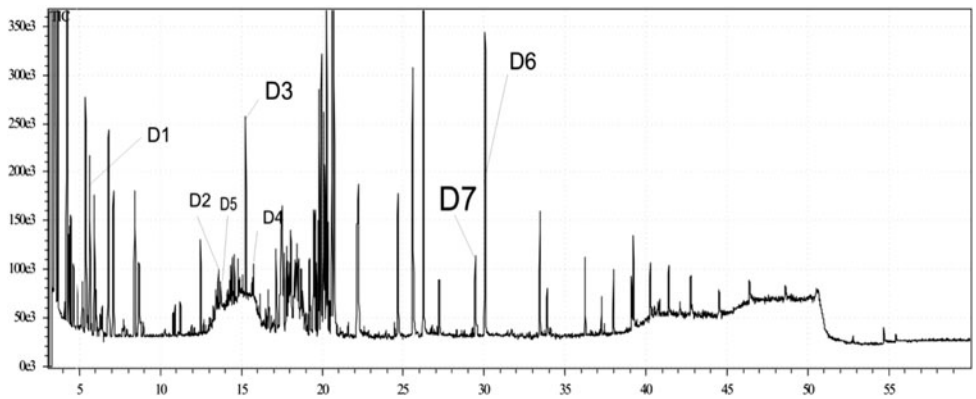

Fig. 6 GC/mass spectrum of RB19 after 20 min of ozonolysis

3.4 Effect of applied voltage, acid type, and concentration

Applied voltage, acid type, and concentration have positive effect on the in situ ozone generation, and these parameters also have influential effect on the ozone concentration. As explained in Sect. 3.1, amount of ozone was increased at 2.4 V versus Ag/AgCl and in 1 M $HClO_4$. Thus, increasing the ozone dose had considerable effect on degradation rate. However, the enhanced ozone concentration increased the driving force for the transfer of ozone from the gas phase into the dye solution. Figure 8 shows that color removal extremely increased with the increasing applied voltage up to 2.4 V in the presence of 1 M $HClO_4$ as electrolyte, so that after ozonolysis for 3 min color removal reached to 100 %. Under these conditions, electrochemical ozone production rate is at the highest value according to the explanation in Sect. 3.1.

Figure 8b shows the effect of acid type on the percentage of color removal. According to the mechanism of ozone reaction with organics in aqueous media, the main oxidants during ozonation could be ozone and hydroxyl radicals. The hydroxyl radicals are formed from the

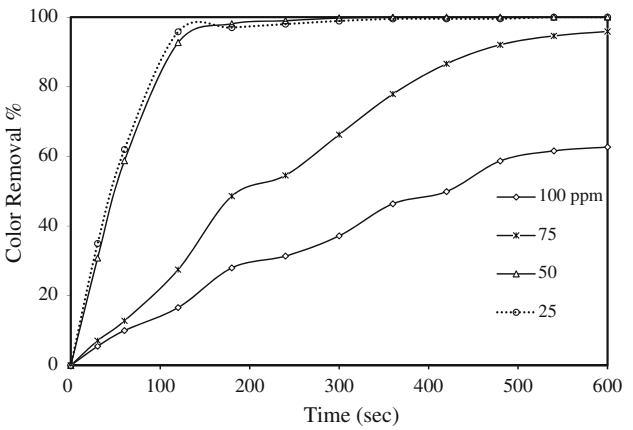

Fig. 7 Effect of initial RB19 concentration on the percentage of color removal

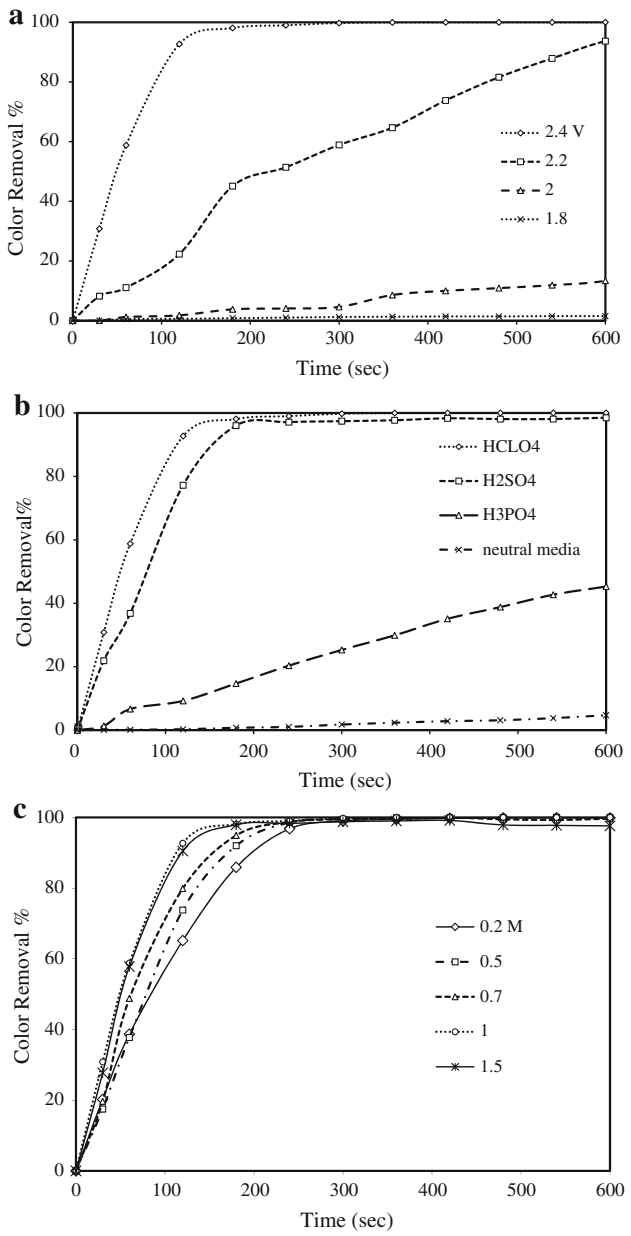

Fig. 8 Effect of **a** applied voltage, **b** different acid type, **c** concentration of $HClO_4$ on the percentage of color removal in 2.4 V versus Ag/AgCl

decomposition of ozone especially at basic pH [33]. Therefore, the direct reaction by ozone molecules is dominated under the acidic conditions, whereas indirect reaction by hydroxyl radicals dominates under basic pH [33]. Thus, the dominated reaction that involves decolorization and degradation of the RB19 chromophores in this research was attributed to the direct reaction of ozone molecules. The type of acid anions had an important effect, evidently causing selective adsorption on electrodes. The highest color removal percent was achieved in $HClO_4$, and the lowest was found in neutral media (dissolved RB19 in deionized water) because in the neutral pH solution, ozone could not produce. Also, Fig. 8 b confirms that acidic media is necessary for ozone generation and directs ozonation.

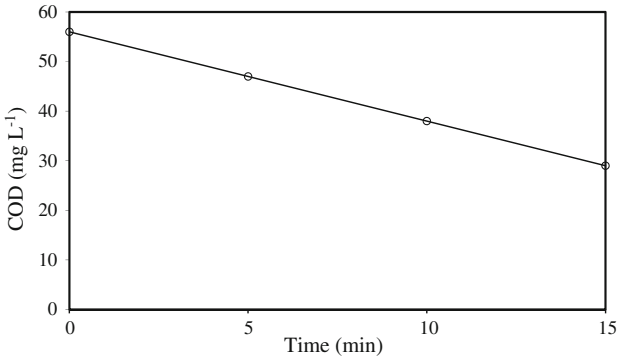

Fig. 9 Effect of reaction time on COD removal

3.5 The evolution of COD removal

Degradation and decolorization of RB19 was further evaluated by COD removal measurement. As shown in Fig. 9, after 3 min of ozonation time, complete decolorization of RB19 was achieved. At this stage and after 15 min reaction time, the percentage of COD removal was 48.2 %. The results show that, during the ozonation process, the easily oxidized reactive dye chromophore and the substances are degraded. The COD removal gave measure of degradation of RB19 and produced intermediates during the dye degradation. Complete removal of the dye is expected to represent the most effective reduction in COD. The amount of COD removal (48.2 %) in our experiments reflects that the mineralization was not completed and the dye was decomposed to small organic substances via ozonation process. The lower COD that compared with the color removal can be explained by incomplete oxidation of organic materials [34].

4 Conclusion

The decolorization and degradation of RB19 was investigated by generated ozone via electrochemical oxidation process. Ozone was generated with high coulombic efficiency via electrochemical oxidation of water on Ni–Sb–SnO_2/Ti electrode at different operating condition. The electrode was characterized by CV and SEM. High concentration of generated ozone was obtained at 2.4 V versus Ag/AgCl in 1 M $HClO_4$ after 10 min electrolysis time. Removal of color and COD were 100 and 48.2 %, respectively. Intermediate compounds were detected by integrated gas chromatography–mass spectrometry (GC/MS). Most intermediates have identified linear structures that are

less harmful to the environment although some aromatic compounds have identified, but their types are low.

References

1. Song S, Ying H, He Z, Chen J (2007) Chemosphere 66:1782
2. Laing I (1991) Rev Prog Color Relat Top 21:56
3. Tan X, Kyaw NN, Teo W, Li K (2006) Sep Purif Technol 52:110
4. Siddique M, Farooq R, Shaheen A (2011) J Chem Soc Pak 33:284
5. Wang B, Kong W, Ma H (2007) J Hazard Mater 146:295
6. Satyawali Y, Balakrishnan M (2008) J Environ Manage 86:481
7. Chatzisymeon E, Xekoukoulotakis NP, Coz A, Kalogerakis N, Mantzavinos D (2006) J Hazard Mater 137:998
8. Parsa JB, Abbasi M (2007) Acta Chim Slov 54:792
9. Gultekin I, Ince N (2006) Ultrason Sonochem 13:208
10. Abbasi M, Asl NR (2008) J Hazard Mater 153:942
11. Lamsal R, Walsh EM, Gagnon AG (2011) Sep Purif Technol 45:3263
12. Javier Benitez F, Acero JL, Real FJ (2002) J Hazard Mater 89:51
13. Panizza M, Cerisola G (2009) Chem Rev 109:6541
14. Neamtu M, Yediler A, Siminiceanu I, Macoveanu M, Kettrup A (2004) Dyes Pigments 60:61
15. Coca M, Pena M, Gonzalez G (2005) Chemosphere 60:1408
16. Swaminathan K, Pachhade K, Sandhya S (2005) Desalination 186:155
17. Song S, Yao J, He Z, Qiu J, Chen J (2008) J Hazard Mater 152:204
18. Wang YH, Cheng SA, Chan KY, Li XY (2005) J Electrochem Soc 152:197
19. Da Silva LM, De Faria LA, Boodts JFC (2003) Electrochim Acta 48:699
20. Konsowa A (2003) Desalination 158:233
21. Peng RY, Fan HJ (2005) Dyes Pigments 67:153
22. Chu W, Ma CW (2000) Water Res 34:3153
23. Wu CH, Kuo CY, Chang CL (2007) React Kinet Catal Lett 91:161
24. Oguz E, Keskinler B (2008) J Hazard Mater 151:753
25. Fanchiang JM, Tseng DH (2009) Chemosphere 77:214
26. Santana MHP, Da Silva LM, Freitas AC, Boodts JFC, Fernandes KC, De Faria LA (2009) J Hazard Mater 164:10
27. Shu HY (2006) J Hazard Mater 133:92
28. Tehrani-Bagha A, Mahmoodi N, Menger F (2010) Desalination 260:34
29. Hsu YC, Chen YF, Chen JH (2004) J Environ Sci Health A 39:127
30. Parsa JB, Abbasi M (2012) J Solid State Electrochem 16:1011
31. Rajkumar D, Song BJ, Kim JG (2007) Dyes Pigments 72:1
32. Oguz E, Keskinler B, Çelik C, ÇelikJ Z (2006) Hazard Mater 131:66
33. Gottschalk C, Libra A, Saupe JA (2000) Ozonation of water and waste water: a practical guide to understanding ozone and its application. Wiley-VCH, Weinheim
34. Sevimli MF, Kinaci C (2002) Water Sci Technol 45:279